Dear Editor and Referee,

We sincerely thank the Reviewer for the careful and constructive assessment of our manuscript entitled "**A Compact Fabry-Perot Interferometer with a Solid Etalon for Measuring Upper Atmospheric Wind and Temperature**". We greatly appreciate your positive assessment of the scientific relevance and instrumental contribution of this work. The comments have helped us improve the clarity, rigor, and presentation of the manuscript.

We have carefully considered each comment and revised the manuscript accordingly. In particular, we re-examined the statistical treatment of the intercomparison and found that several quantities previously labeled "mean absolute difference" were, in fact, signed mean differences (biases). This terminology error and the associated combination of the two wind components have been corrected throughout, and we now report consistent statistics for each comparison. This correction is described in detail under Major Comment 1 and is reflected in the abstract, Section 5.1, Figures 7 and 9, and the conclusions. Our detailed responses are provided below. The Reviewer's comments are reproduced ***in bold and italics***. Our responses and descriptions of the corresponding revisions are in blue. Revisions in the manuscript are marked in purple.

This manuscript describes a Fabry–Perot interferometer employing a 70-mm fused-silica solid etalon, including its optical design, retrieval model, laboratory AOFS tests, and comparisons with a collocated DCOI and a conventional FPI at another site. The use of a solid etalon for ground-based thermospheric airglow measurements has practical interest. Combining laboratory calibration with sustained field observations is a strength of the study.

Major comments:

Comment 1: In Figure 7, the DCOI comparisons have μ values of 1.35 and 2.40 m/s but standard deviations of 20.49 and 19.73 m/s. The XLO comparisons have μ values of 4.92 and 6.23 m/s. The text calls some of these values mean absolute differences, whereas the figure labels them only as μ. The overall values of 1.88 and 5.58 m/s are the unweighted averages of the respective component μ values, despite unequal sample counts. These appear more consistent with signed mean differences than MAEs and require verification.

Response: We thank the Reviewer for this very helpful suggestion. We re-examined the statistics and confirm that the quantities labeled μ in Figure 7 are signed mean differences (biases). That is to say, these quantities are the mean of the paired differences between the two compared instruments, and not the mean absolute differences (MAEs). We want to express our sincere apologies for the inaccuracy concerning the "mean differences" in the main text, which were erroneously referred to as "mean absolute differences". In the Abstract and Conclusions, we intended to report the mean value of the mean differences between the meridional and zonal wind components. Therefore, we have revised all

ambiguous expressions in the revised manuscript to clarify their intended meaning, as detailed below. Concurrently, we carefully inspected and verified each parameter shown in Figures 7 and 9. We discovered an error in the RMSE value for plane (a) in Figure 7, and we have corrected it in the revised manuscript.

Lines 20-23: "Statistical analysis yielded a mean difference (DCOI/FPI - SEFPI), averaged across both meridional and zonal wind components, of +1.88 m/s relative to the co-located DCOI instrument and +5.58 m/s relative to the conventional FPI located 502 km away. Temperature comparisons between the two FPIs revealed a correlation coefficient of 0.86, with a mean difference (FPI - SEFPI) of +62.38 K."

Lines 286-287: "When the two horizontal wind components are considered together, the average of the mean difference was +1.88 m/s."

Lines 369-370: "When both horizontal wind components are considered, the average of the mean differences (DCOI/FPI - SEFPI) is +1.88 m/s relative to the DCOI and +5.58 m/s relative to the FPI."

Comment 2: The instruments differ in scan timing, field of view, and sampling volume, and SIZW and XLO are separated by 502 km. Although these differences are acknowledged, the matching of 26-minute and 31-minute measurements to SEFPI is insufficiently described, as are horizontal-wind reconstruction, vertical-wind treatment, and quality control. Averaging temperatures over five directions also mixes spatially and temporally distinct measurements.

Response: Thank you for your constructive comments. We agree that these methodological details are important for ensuring the reproducibility of the analysis. Accordingly, we have expanded the description of the cross-comparison procedure in Section 5 to clarify the observation cadence, temporal matching, horizontal-wind reconstruction, treatment of vertical winds, and quality-control criteria.

For the wind cross-comparison, the three instruments have different temporal resolutions. For example, the DCOI and SEFPI instruments at the SIZW station have an observation cadence of approximately 26 min, whereas the FPI at the XLO station has a cadence of approximately 31 min. To ensure temporal consistency, the meridional and zonal wind measurements from the DCOI and XLO FPI were linearly interpolated to the corresponding SEFPI observation times before the cross-comparison. Regarding the reconstruction of horizontal winds, we adopted the assumption of zero nightly mean vertical wind, following Harding et al. (2014). The line-of-sight (LOS) wind measurements were subsequently resolved into horizontal wind components using the geometric relationship among the LOS, horizontal, and vertical wind components described by Vasilyev et al. (2017).

We also appreciate the Reviewer's concern regarding the potential influence of spatial and temporal variations when averaging temperatures measured in the five viewing directions. We acknowledge that measurements from different directions may sample distinct spatial regions and correspond to different observation times. To minimize temporal inconsistencies, we first linearly interpolated the temperature measurements from the five viewing directions of each instrument to common time points and then

calculated the directional average at each time point. Subsequently, the resulting mean temperature time series from the two instruments were independently interpolated to common time points to ensure temporal alignment for the cross-comparison.

To further evaluate the potential influence of directional variability, we examined the temperature dispersion among the five viewing directions of each instrument at individual time points and compared it with the mean absolute temperature difference between the two instruments. As shown in Figure 8 of the revised manuscript, the error bars represent the standard deviations of the temperatures measured in the five directions, thereby characterizing the directional dispersion within each instrument. Except for the period around midnight, the directional temperature dispersion is consistently smaller than the mean temperature difference between the two instruments. It suggests that during most of the observation period, the temperature variability among the five viewing directions within each instrument is relatively small compared with the temperature differences between instruments. It should also be noted that the two instruments are deployed at different stations separated by approximately 500 km. Consequently, their temperature differences may also reflect regional-scale spatial variability over a much larger spatial scale than that sampled by the five viewing directions of an individual instrument. Taken together, these results suggest that directional averaging has a relatively limited influence on the overall temperature cross-comparison during most of the observation period. Nevertheless, some local spatial and temporal variations may be smoothed out through the averaging process.

We acknowledge, however, that the current approach cannot fully resolve the spatial representativeness of the measurements or eliminate the effects of spatial and temporal variability. Future observations with both instruments deployed at the same station will enable direction-by-direction temperature comparisons under more consistent spatial conditions, allowing a more rigorous assessment of their measurement consistency and their respective capabilities in resolving spatial and temporal temperature variations.

Finally, to help readers understand the text more easily, a detailed description of the comparative data processing has been added to Section 5 of the revised manuscript.

Lines 227-245: “Before cross-comparison, the SEFPI, DCOI, and FPI observations were independently quality-controlled by removing measurements affected by cloud, precipitation, and moonlight contamination, as identified using cloud-sensor measurements and all-sky airglow images. In particular, the methodology described by Li et al. (2021) was adopted to identify and extract clear-sky observations from cloud sensor data. To mitigate moonlight contamination, a 37° exclusion threshold was applied to the angular separation between the Moon and the instrument's line-of-sight, based on the instrument's FoV and aperture. Following daily data screening, DCOI wind retrievals with uncertainties exceeding 75 m/s were excluded. This threshold was determined by the retrieval method and does not directly represent the actual wind measurement errors. For the SEFPI and XLO FPI, only measurements with quality flags of 0 and 1 were retained for subsequent analysis. At low and middle latitudes, thermospheric winds are commonly assumed to be spatially uniform across the four azimuthal viewing directions, while the mean

vertical wind over an entire nighttime observing period is assumed to be zero (Harding et al., 2014; Makela et al., 2011; Tesema et al., 2017). Under these assumptions, the horizontal wind vector for each viewing direction was reconstructed from the line-of-sight wind using the method described by Vasilyev et al. (2017).

For the wind comparison, the northward and southward vector winds were first interpolated to common observation times and then averaged to obtain the representative meridional wind. The eastward and westward vector winds were processed similarly to derive the representative zonal wind. For the SEFPI and FPI temperature measurements, observations from the five viewing directions were first interpolated to a common reference time (i.e., the zenith observation time) and then averaged to obtain the representative temperature. To account for the different temporal sampling cadences of the three instruments, the DCOI and XLO FPI measurements were linearly interpolated to the corresponding SEFPI observation times before inter-instrument comparisons of both wind and temperature measurements."

Lines 318-327: "To assess the potential influence of spatial variability from averaging the five viewing directions, the standard deviation of the temperatures measured in the five directions at each time point for both instruments was calculated. The error bars in Figure 8 represent these standard deviations and characterize the temperature dispersion among the five viewing directions. Except for the period around midnight, the directional temperature dispersion was consistently smaller than the mean temperature difference between the two instruments. This finding indicates that, during most of the observation period, the temperature variability among the five viewing directions within each instrument was comparatively minimal relative to the inter-instrument temperature difference. Despite the approximately 502 km separation between the two instruments, which sample distinct atmospheric volumes, the modest directional dispersion suggests that aggregating the five viewing directions had a negligible effect on the overall temperature comparison during most observation periods. However, this averaging procedure may have smoothed out some local spatial and temporal variations."

Lines 397-401: "Future work will focus on co-locating the SEFPI and the XLO FPI at the same site for direct measurement validation, including direction-by-direction temperature comparisons to characterize better spatial variability that the current directional averaging approach cannot fully resolve. In addition, a narrower-bandwidth interference filter will be employed in the SEFPI to investigate the observed temperature discrepancies further."

Reference

Harding, B. J., Gehrels, T. W., and Makela, J. J.: Nonlinear regression method for estimating neutral wind and temperature from Fabry–Perot interferometer data, Appl. Opt., 53, 666–673, https://doi.org/10.1364/AO.53.000666, 2014.

Vasilyev, R. V., Artamonov, M. F., Beletsky, A. B., Zherebtsov, G. A., Medvedeva, I. V., Mikhalev, A. V., and Syrenova, T. E.: Registering Upper Atmosphere Parameters in East Siberia with Fabry–Perot Interferometer Keo Scientific "Arinae," Solar-Terrestrial Physics, 3, 61–75,

https://doi.org/10.12737/szf-33201707, 2017.

Minor comments:

Comment 1: line 101 calls 0.0001°C a mean absolute deviation, whereas Appendix A1 describes a signed mean deviation. Verify the definition and make the text, appendix, and caption consistent.

Response: Thank you for your careful review and helpful suggestion. We have verified that 0.0001 °C represents the signed mean deviation of the measured etalon temperature from the 30 °C set point, rather than the mean absolute deviation. Therefore, we have corrected the terminology at line 101 and ensured consistency throughout the main text, Appendix A1, and the caption of Figure A1. The revised sentence reads:

Lines 101-103: "During the 36 effective nighttime field observation periods, the measured etalon temperature showed a mean deviation of 0.0001 °C from the set point, with a standard deviation of 0.0026 °C (see Appendix, Figure A1)."

Lines 417-418: "The mean deviation was 0.0001 °C, with a standard deviation of 0.0026 °C."

Comment 2: Table 1, and Equations 1–2: provide measured FSR, effective finesse, instrumental line width, and uncertainties at 630.0 and 632.8 nm. Explain the treatment of adjacent orders or periodic line extension when integrating over one FSR in Equation 2, and test the integration-range sensitivity of the temperature retrieval.

Response: We thank the Reviewer for raising this important technical point. Because temperature is retrieved from Doppler broadening and the instrumental line width of the solid etalon constitutes a substantial fraction of the intrinsic width of the OI 630.0 nm emission line, the temperature retrieval is sensitive to both the instrument function and the integration range. We have addressed all three points.

First, we performed ten independent inversions of the laser calibration interferograms, with the laser wavelength fixed at 632.8 nm and the refractive index fixed at 1.457. The resulting etalon thickness was 15.9998734 mm ± 0.056 nm. It corresponds to a free spectral range (FSR) of 0.21448 ± 0.00001 cm^{-1}, equivalent to wavelength intervals of 8.589 pm at 632.8 nm and 8.513 pm at 630.0 nm. The fitted reflectivity was 0.78155 ± 0.0013, yielding a reflective finesse of 12.7 ± 0.1. After accounting for the effect of the λ/100 surface flatness, the effective finesse was determined to be 12.3 ± 0.1. It corresponds to an instrumental line width of 0.01744 ± 0.0001 cm^{-1}, equivalent to 0.70 pm at 632.8 nm and 0.69 pm at 630.0 nm, with a wavelength uncertainty of approximately ±0.004 pm. These experimentally determined parameters are now reported in Table 2 of the revised manuscript.

Line 170:

Table 2. Measured technical parameters of the SEFPI from laser calibration

Parameters	*Specifications*
Free Spectral Range (cm^{-1})	0.21448 ± 10^{-5}
Effective Finesse	12.3±0.1
Instrument Line Width (cm^{-1})	0.01744 ± 10^{-4}

Second, we agree with the Reviewer that Eq. (4) in the original manuscript specifies an integration interval spanning exactly one FSR, from $\lambda_0 - \delta\lambda_0/2$ to $\lambda_0 + \delta\lambda_0/2$. We should have explicitly stated that in the numerical implementation, the convolution is actually performed over four FSRs. Thus, the original equation represented only the minimum periodic integration interval rather than the full integration range used in the numerical calculations. No periodic folding of the source spectrum is performed in our implementation; therefore, no additional extension of the integrand is required. To clarify this distinction and avoid ambiguity, we have introduced the number of FSRs, N, as an explicit parameter in Eq. (4). The revised equation is now given as follows (line 152):

$$Y(r) = \int_{\lambda_0 - N\cdot\delta\lambda_0/2}^{\lambda_0 + N\cdot\delta\lambda_0/2} \tilde{A}(r,\lambda)E(\lambda)\mathrm{d}\lambda + B_{ccd} \quad (1)$$

The text following the equation has also been revised to clarify that:

Lines 153-158: "Where λ_0 is the central wavelength of nightglow emission, $\delta\lambda_0$ represents the free spectral range (FSR), N is the number of FSRs spanned by the integration window, and B_{ccd} is the CCD detector bias. As the Airy function is periodic in wavelength with a period of FSR, the integration window is defined to span an integer number of FSRs. It ensures that the convolution accounts for complete interference orders without introducing partial orders at either boundary. The window must also be sufficiently wide to encompass the full Doppler-broadened emission line. As a result, N=4 is adopted to ensure adequate coverage of the line profile across the temperature range expected under both low- and high-solar-activity conditions."

Finally, we performed the sensitivity test requested by the Reviewer, and the results are presented in Figure 1 below. The test confirms that the one-FSR integration window specified in the original Eq. (4) is insufficient to ensure accurate temperature retrievals, which motivated our use of a four-FSR window in the numerical implementation.

To assess the sensitivity of the retrievals to the integration range, we generated noise-free synthetic interferograms using the forward model described in Section 3. Subsequently, we inverted them using integration windows spanning 0.5-4 FSR, while keeping all other parameters fixed. The temperature sensitivity was evaluated at 600, 800, 1000, 1200, 1400, and 1600 K, with an LOS wind speed of 0 m/s. The wind sensitivity was assessed for LOS velocities ranging from −200 to +200 m/s in increments of 50 m/s, with the temperature fixed at 1000 K.

The results demonstrate that the retrievals are fully converged for integration windows of 2 FSR or wider, with maximum differences of 1.3 K in temperature and 0.15 m/s in LOS wind across all tested cases. For

a 1.5-FSR window, the differences remain within 12 K in temperature (within 1.1 K for temperatures of 1200 K and below) and 0.2 m/s in LOS wind. In contrast, the 1.0-FSR window leads to substantial temperature underestimation, with errors of 41 K at 1000 K and 267 K at 1600 K, although the LOS wind is still retrieved to within 3 m/s of its prescribed value. The 0.5-FSR window results in retrieval failure; the retrieved temperatures collapse to 175-290 K, largely independent of the prescribed temperatures, while the LOS wind error increases to 111 m/s.

Throughout this study, we therefore adopt a four-FSR integration window, which is twice the minimum range required to achieve convergence within 1.5 K. The residual systematic errors associated with the integration range are consequently limited to less than 1 K in temperature and 0.15 m/s in LOS wind, making them negligible compared with the overall retrieval uncertainties reported in this study. Moreover, the choice of integration range does not affect any of the main conclusions.

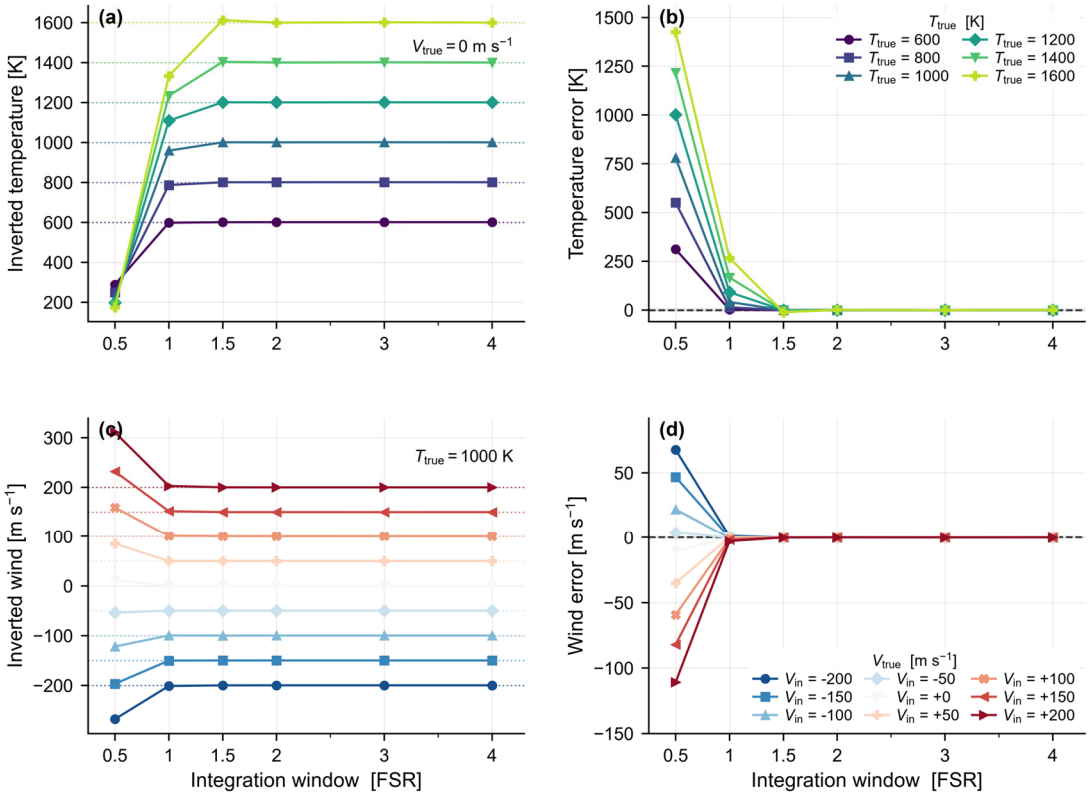


Figure 1. Retrieved temperature (a) and line-of-sight wind (c), together with their errors (b, d), as a function of the integration window of the forward model, with n = 1.457, d = 16 mm (FSR = 8.513 pm). Colors in (a, b) denote the true temperature (600 to 1600 K) and in (c, d) the true wind (−200 to 200 m/s); dotted lines mark the true values, and grey bands in (b, d) indicate ±10 K and ±1 m/s. Windows narrower than 1.5 FSR truncate the emission line and bias both quantities; 2 FSR or wider is needed for convergence.

Comment 3: The text and appendices refer to 36 effective nights, whereas Figures 5 and 6 display 30 nights. Explain the displayed, screened, and statistically analyzed subsets, give the exact dates of the 54-day campaign, and define μ, σ, N, and error bars in Figures 7 and 9.

Response: We have clarified the data-screening procedure and added the exact observation dates and definitions of the symbols used in the revised manuscript. We have also clarified the apparent discrepancy between the 36 effective SEFPI observing nights reported in the text and the 30 nights shown in Figures 5 and 6. Specifically, the 36 nights represent the total number of nights with valid SEFPI observations, comprising 24 nights with simultaneous observations from all three instruments, 6 additional nights with SEFPI-DCOI observations only, and another 6 nights with SEFPI-FPI observations only. In contrast, Figures 5 and 6 each include 30 nights corresponding to the available observations for the respective instrument pair (24 nights of three-instrument observations plus 6 nights of pair-specific observations). The revised text in Section 5 reads as follows:

Lines 209-210: "Field observations were conducted over a period of 54 days, from 14 March to 6 May 2024, at the Siziwang (SIZW) station (geog.: 41.5°N, 111.7°E; geom.: 36.9°N) in the north of China."

Lines 246-251: "During the 54-day campaign, the SEFPI was observed effectively on 36 nights, including 24 nights with valid simultaneous data from all three instruments (SEFPI, DCOI, and XLO FPI), 6 nights with valid SEFPI and DCOI data only, and 6 nights with valid SEFPI and FPI data only. Consequently, the SEFPI-DCOI and SEFPI-FPI intercomparisons each comprise 30 nights. Before analyzing the horizontal wind measurements of the SEFPI, the reliability of the retrieved wind zero point was evaluated using zenith observations. Analysis of quality-controlled zenith vertical wind measurements from the SEFPI over the 36 effective nights showed no appreciable systematic offset from zero (see Appendix, Figure A2)."

The captions of Figures 7 and 9 have been updated as follows:

Lines 300-303: "Figure 7. Statistical comparison of horizontal wind measurements. Panels (a) and (b) show the meridional and zonal wind comparisons between the SEFPI and DCOI, respectively, while panels (c) and (d) show the corresponding comparisons between the SEFPI and XLO FPI. In each subpanel, μ denotes the signed mean difference, σ is the standard deviation of the differences, N represents the number of paired samples, and RMSE shows the root mean square error."

Lines 343-345: "Figure 9. Statistical comparison of temperature measurements between the SEFPI at the SIZW station and the FPI at the XLO station, following the format of Figure 7. μ denotes the signed mean difference, σ is the standard deviation of the differences, N represents the number of paired samples, and RMSE shows the root mean square error."

Comment 4: Page 14, lines 373–375: in addition to the DCOI portal and SEFPI dataset, give a specific source or access procedure for the XLO reference data, paired observation catalog, quality flags to reproduce the statistics and Figures 4–9.

Response: We thank the Reviewer for pointing this out. We have revised the data-availability information to ensure that all three datasets and the intercomparison statistics can be accessed and used to reproduce the results presented in this study. Specifically, the XLO FPI reference data, together with a detailed data description, have been added to the existing Zenodo record of Wang (2026), alongside the SEFPI datasets. Accordingly, the Zenodo DOI has been updated from 10.5281/zenodo.22030313 to 10.5281/zenodo.23664978 in the revised manuscript (line 627). The revised Data Availability section (lines 438-439) reads as follows:

"The SEFPI and the XLO FPI datasets for this study can be accessed via the website link provided by Wang (2026)."

Comment 5: Page 9, line 245: replace "considered tighter" with "considered together." Distinguish lower signed wind velocities from smaller wind magnitudes. The Makela et al. (2009a, 2009b) entries on p. 17 have identical titles and DOIs and should be checked for duplication.

Response: Thank you for your careful review and helpful suggestions. We have addressed all three points as follows.

First, we confirm that "considered tighter" in section 5.1 was a typographical error and have corrected it to "considered together" (line 287).

Second, we have clarified the terminology to distinguish between signed wind velocities and wind magnitudes. In Figure 7, the SEFPI measurements are plotted on the x-axis, while the corresponding DCOI or FPI measurements are plotted on the y-axis. Therefore, a fit slope greater (less) than 1.0 indicates that the DCOI or FPI reports larger (smaller) wind magnitudes than the SEFPI. Accordingly, the slopes of 1.15 and 1.01 in the DCOI comparison indicate that the SEFPI generally reports slightly smaller wind magnitudes than the DCOI. In contrast, the slopes of 0.88 and 0.89 in the FPI comparison indicate that the SEFPI reports larger wind magnitudes than the FPI.

The mean differences (DCOI/FPI-SEFPI), which characterize the signed velocity offsets rather than differences in wind magnitudes, are reported separately. These differences are positive for both comparisons: +1.35 and +2.40 m/s for the meridional and zonal components, respectively, in the DCOI comparison, and +4.92 and +6.23 m/s, respectively, in the FPI comparison. This indicates that both the DCOI and FPI measurements are, on average, shifted toward more positive wind velocities relative to the SEFPI measurements. We have revised the relevant descriptions in Sections 5.1, the Abstract, the Discussion, and the Conclusions accordingly.

Lines 280-285: "The fit slopes are 1.15 for the meridional component and 1.01 for the zonal component, indicating generally good consistency in wind variability between SEFPI and DCOI. This finding also

shows that the DCOI wind measurements in magnitude are slightly higher than those from the SEFPI measurements. The mean differences (DCOI - SEFPI) are +1.35 m/s for the meridional component and +2.40 m/s for the zonal component, suggesting that the DCOI measurements are, on average, shifted toward more positive wind velocities relative to the SEFPI measurements."

Lines 289-293: "The fit slopes are 0.88 for the meridional component and 0.89 for the zonal component, both below 1.0, indicating that the magnitude of the SEFPI winds is slightly larger than that of the FPI. The mean differences (FPI - SEFPI) are +4.92 m/s for the meridional component and +6.23 m/s for the zonal component, with a standard deviation of 17.66 m/s and 16.79 m/s, respectively. Therefore, the SEFPI measurements are, on average, shifted toward more negative wind velocities relative to the FPI measurements."

Finally, we confirm that the entries for Makela et al. (2009a) and Makela et al. (2009b) referred to the same publication, with identical titles, authors, journal information, page numbers, and DOI. We have therefore merged them into a single reference, "Makela et al. (2009)," and corrected the corresponding in-text citations. In addition, the citation supporting the discussion of etalon thermal stability has been replaced with an appropriate, distinct reference, as indicated in the revised reference list.

Lines 582-584: "Rees, D., Fuller-Rowell, T. J., Lyons, A., Killeen, T. L., and Hays, P. B.: Stable and rugged etalon for the Dynamics Explorer Fabry-Perot interferometer 1: Design and construction, Appl. Opt., 21, 3896–3902, https://doi.org/10.1364/AO.21.003896, 1982."

We believe these changes substantially improve the rigor and reproducibility of the manuscript.

Sincerely,

The Authors